Refereed Proceedings

The 12th International Conference on Fluidization - New Horizons in Fluidization Engineering

Engineering Conferences International *Year* 2007

A Rotating Fluidized Bed in a Static Geometry: Experimental Proof of Concept

Juray De Wilde* Luc Wautier† Guy B. Marin‡
Geraldine J. Heynderickx** Axel de Broqueville††

*Université Catholique de Louvain, Belgium, dewilde@imap.ucl.ac.be
†Université catholique de Louvain
‡Ghent University
**Ghent University
††

A ROTATING FLUIDIZED BED IN A STATIC GEOMETRY: EXPERIMENTAL PROOF OF CONCEPT

Juray De Wilde[1,*], Luc Wautier[1], Guy B. Marin[2], Geraldine J. Heynderickx[2], Axel de Broqueville

1(*). Corresponding author, Department of Materials and Process Engineering, Université catholique de Louvain, Réaumur, Place Sainte Barbe 2, B-1348 Louvain-la-Neuve, Belgium
T: +32 10 47 8193, F: +32 10 47 4028, E: dewilde@imap.ucl.ac.be

2. Laboratorium voor Petrochemische Techniek, Ghent University, Krijgslaan 281, blok S5, B-9000 Gent, Belgium

ABSTRACT

The new concept of a rotating fluidized bed in a static geometry (RFB-SG) is presented (1). The rotating motion of the particle bed and the tangential fluidization of the solids are obtained by the tangential injection of the fluidization gas via multiple gas inlet slots in the outer cylindrical wall of the fluidization chamber. The new fluidization concept is experimentally investigated and proven using either large diameter, low density polymer particles or small diameter, higher density Alumina particles.

INTRODUCTION

In so-called rotating fluidized beds (RFB), a radially outwards centrifugal force exerted on the solids is balanced by a radially inwards gas-solid drag force. The latter results from a radially inwards moving fluidization gas. Due to the centrifugal force, the rotating fluidized bed has a cylindrical shape. Rotating fluidized beds have flow characteristics that are advantageous over those of conventional (i.e. gravitational) fluidized beds for a variety of applications (2,3). In fact, almost any advantage of the conventional fluidized beds is maintained or increased.
The centrifugal force is determined by the rotational speed of the particle bed and can be a multiple of earth gravity, allowing a vertical or horizontal operation, much higher fluidization gas velocities and increased (radial) gas-solid slip velocities. The latter is expected to significantly improve the inter-phase mass and heat transfer. Therefore, rotating fluidized beds are potentially advantageous for use with exothermic / endothermic reactions (3) or for drying applications. Due to the centrifugal force, excellent gas-solid separation can be obtained, despite higher fluidization gas velocities (4). High rotational speeds are reported to allow more gas throughput without serious formation of bubbles or a slugging bed. This allows for example to increase the efficiency and improve the flexibility of gas phase polymerization reactors (3). The cylindrical shape of the rotating fluidized bed allows a very high ratio between its freeboard surface and its thickness (height in

The 12th International Conference on Fluidization - New Horizons in Fluidization Engineering, Art. 70 [2007]

conventional fluidized beds) and a more compact construction. Rotating fluidized beds have attracted special interest recently, due to their advantages in fluidizing very fine particles, such as cohesive (Geldart group C) micro- and nano-particles (2,5,6,7).

The centrifugal force requires a rotating motion. In the rotating fluidized beds investigated so far (named conventional rotating fluidized beds in what follows) (2-11), a motor is used to rotate the reactor or fluidization chamber fast around its axis of symmetry. The fluidization gas is radially introduced in the fluidization chamber by means of gas distributors in the rotating outer cylindrical wall of the fluidization chamber. Usually a porous or sintered wall is used (2,4,5,6,8,9). Slotted gas distributors have been studied as well (8). Obvious disadvantages of the conventional rotating fluidized bed technology are the use of a motor and the moving geometry, i.e. the rotating fluidization chamber. The latter may be at the origin of mechanical vibrations and makes sealing and particle feeding / removal to / from the fluidization chamber challenging. To overcome these difficulties, the new concept of a rotating fluidized bed in a static geometry (RFB-SG) is proposed and investigated with two types of particles.

THE CONCEPT OF A ROTATING FLUIDIZED BED IN A STATIC GEOMETRY

To induce a rotating motion in the static geometry, the fluidization gas is injected tangentially via multiple gas inlet slots at the outer cylindrical wall of the fluidization chamber (Figure 1(a)). As a result of the tangential gas-solid drag force, the solid particles in the fluidization chamber rotate as well and experience a radially outwards centrifugal force. By the action of the centrifugal force, the particles tend to form a rotating particle bed against the outer cylindrical wall of the fluidization chamber. The tangential gas-solid slip velocity is expected to be small ($v_t \approx u_t$), in contrast to the radial gas-solid slip velocity. The gas is moving radially inwards (Figure 1(b)), forced to leave the fluidization chamber via an inner chimney with one or multiple outlet slots (Figure 1(a)). The solids experience a radially inwards gas-solid drag force counteracting the radially outwards centrifugal force. The relative importance of the two forces depends on the operating conditions and on the fluidization chamber design, in particular its outer and inner diameters and the number of gas inlets, their surface area, and eventually their angle of injection. A proper fluidization chamber design allows to balance the centrifugal force and the drag force (Figure 1(a) and (b)) and the radial fluidization of the rotating particle bed.

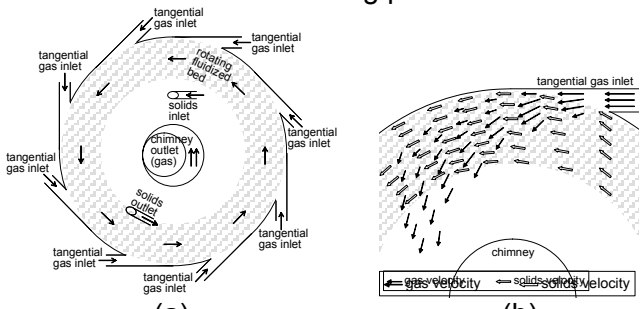

(a) (b)

Figure 1: Schematic representation of the concept of a rotating fluidized bed in a static geometry (RFB-SG). (a) 2D section of the fluidization chamber; (b) Detail of the gas and solids velocity behavior near a tangential gas inlet of the fluidization chamber.

The use of slotted gas distributors in conventional rotating fluidized beds resulted in non-uniform fluidization and restructuring of the fluidized bed, the fluidization occurring primarily over the slots (8). In the new rotating fluidized bed in a static geometry, the non-uniformity introduced by slotted gas distributors is much less pronounced due to the tangential distribution of the gas over the fluidized bed.
It should be emphasized that the gas injected in the fluidization chamber exerts both a tangential and a radial force on the particles. As such, the gas injected serves both as the driving power for the rotational motion in the fluidization chamber and as fluidization gas. The tangential and radial motion of the gas in the fluidization chamber implies, however, a combined tangential and radial fluidization of the particle bed. Whereas in the radial direction, the centrifugal force is to be balanced by the radial drag force, in the tangential direction the shear stress counteracts the tangential drag force.

EXPERIMENTAL SET-UP

The experimental set-up at UCL-IMAP is shown in Figure 2 and consists of a compressor, a gas distribution device, a rotary valve, a solids container and feeder, the rotating fluidized bed apparatus, a cyclone, a filter, and a solids recuperator. The rotating fluidized bed apparatus, the cyclone, and the filter can be rotated around an axis, so that the fluidization chamber can be operated in the horizontal or the vertical (Figure 2) position. The rotating fluidized bed apparatus is constructed from three coaxial cylinders, which separate the medium fluidization chamber or reactor from the outer gas distribution chamber and from the inner chimney. As seen in Figure 3, the cylindrical design of the fluidization chamber is approximated by a polygonial design in the present investigation.
The compressor delivers a maximum air flow rate of 0.33 $Nm^3\ s^{-1}$ and a maximum pressure of 1.8 bar. Due to the pressure drop in the gas distribution section, the fluidization chamber, the cyclone, and the filter, the actual maximum gas flow rate through the experimental set-up is $\pm$ 0.2 $m^3\ s^{-1}$. The gas flow rate to the fluidization chamber can be controlled with a rotary valve. From the gas distribution device, the gas enters the 36 cm diameter, 13.5 cm long fluidization chamber via 12 tangential 4 mm width gas inlet slots in the cylindrical outer wall of the fluidization chamber.
The solids flow rate is controlled by a volumetric screw feeder and a sealing rotary valve. The solids are pneumatically conveyed to the fluidization chamber, which they enter via a solids inlet tube in one of the plexi-glass end plates. Radially, the solids inlet tube is positioned such that the solids enter in the dilute part of the fluidization chamber. To facilitate the tangential acceleration of the solids, the solids are fed in the tangential flow direction and the solids inlet tube makes a 30° angle with the plexi-glass end plate. The gas and eventually some solids (losses, fines) leave the fluidization chamber via an inner, quasi-centrally positioned, $\pm$ 12 cm diameter chimney with, in the present case, a single, 9 cm width, outlet slot. Multiple outlet slots could be used as well. The gas that is removed from the fluidization chamber via the chimney is sent to a cyclone and a bag filter to remove eventual solids from the gas stream before sending it to the vent. The solids are removed from the fluidization chamber via a solids outlet tube in one of the plexi-glass end plates of the fluidization chamber. Radially, the solids outlet tube is positioned near the fluidized bed free-board. To facilitate the solids outflow, the solids outlet tube is oriented in the tangential flow direction, making a 30° angle with the plexi-glass end plate. The solids are transported via a transfer leg to an expansion vessel where

The 12th International Conference on Fluidization - New Horizons in Fluidization Engineering, Art. 70 [2007]

Table 1: Experimental conditions

	Unit	Value
Fluidization chamber diameter	[m]	$36 \cdot 10^{-2}$
Fluidization chamber length	[m]	$13.5 \cdot 10^{-2}$
Chimney diameter	[m]	$\pm 12 \cdot 10^{-2}$
Number of tangential gas inlet slots	[/]	12
Gas inlet slot width	[m]	$4 \cdot 10^{-3}$
Total gas flow rate	[$m^3 s^{-1}$]	0.2
Number of chimney outlet slots	[/]	1
Chimney outlet slot width	[m]	$9 \cdot 10^{-2}$
Outlet pressure	[Pa]	101300
Temperature	[K]	333
Number of solids inlets and outlets	[/]	1 / 1, via opposite end plates
Particle material	[/]	a) polymer b) Alumina
Average particle size	[m]	a) $2 \cdot 10^{-3}$ (length) - $5 \cdot 10^{-3}$ (diameter) (cylinders) b) $300 \cdot 10^{-6}$ (original); $400 \cdot 10^{-6}$ (fluidization chamber) (Figure 14)
Particle density	[kg m^{-3}]	a) 950 b) 2100
Solids loading	[kg]	a) 0 - 2 b) 0 - 1.5
Rotational speed (estimated)	[rps]	a) 3-6 b) 3-7

Figure 2: Experimental set-up. (Vertical position shown.)
Right: solids container and feeder; Centre: from bottom to top: rotating fluidized bed apparatus, cyclone, bag filter; Back: gas distribution device; Left: solids recuperator.

they are recuperated. Neglecting solids losses via the chimney, the solids residence time in the fluidization chamber can be freely chosen and adjusted by controlling the solids inlet and outlet flow rate. The gas flow rate and the solids feeding / removal rate hardly influence the fluidized bed thickness or "height" (in the radial direction) that can be achieved, which is mainly determined by the solids outlet position.
With one and the same fluidization chamber design, the fluidization behavior with two different types of solids is investigated. The solid particle characteristics are summarized in Table 1. The 5 mm diameter, 2 mm long cylindrical polyethylene polymer particles with a particle density of 950 kg m^{-3} behave like Geldart D-type particles in the earth gravitational field (1G). It should be stressed that particles may behave like a different Geldart-type in a centrifugal field (7). The Alumina particles have a mean particle size of 300 μm and a particle density of 2100 kg m^{-3} and behave like Geldart B-type particles in the earth gravitational field (1G). It should be noted that during continuous operation with the Alumina particles, the mean particle size in the fluidization chamber was measured to be 400 μm rather than 300 μm, due to a preferential loss of fines via the chimney.
The fluidization behavior is studied visually and using normal and fast digital cameras. The solids feeding rate, the solids losses via the central chimney, and the amount of solids recuperated via the solids outlet are measured, allowing to determine the solids hold-up in the fluidization chamber. The total gas flow rate, the pressure, and the temperature are measured immediately upstream of the gas distribution device.
Experiments start with an empty fluidization chamber. First, the gas flow rate to the fluidization chamber is set. Next, the particles are fed to the fluidization chamber (if

wanted step wise) at a known flow rate. The fluidization chamber gradually fills with particles. If the solids outlet is open, particles start leaving the fluidization chamber via the solids outlet and a continuous, quasi-steady regime can be reached. If the solids outlet is closed, the fluidization chamber can be filled with particles up to the level where particles are lost via the central chimney outlet. Alternatively, with a closed solids outlet, the solids feeding can be stopped before losing particles via the chimney. Experiments can then be carried out with any chosen residence time of the particles in the fluidization chamber.

FLUIDIZATION BEHAVIOR WITH POLYMER PARTICLES

Experiments are carried out with the solids outlet closed. The fluidization chamber is gradually filled with polymer particles (a) in Table 1) at an almost constant total gas flow rate, which approaches the maximum possible total gas flow rate of about 0.2 m^3 s^{-1}. From fast digital camera pictures taken at 1000 frames per second, the rotational speed of the fluidized bed is estimated between 3 and 6 rps, respectively for the highest and the lowest solids loading. At the outer cylindrical wall of the fluidization chamber, the corresponding centrifugal acceleration is roughly between 7 and 26 G. The rotational speed of the fluidized bed could be adapted by changing its driving force, i.e. the gas flow rate.

The behavior of the rotating fluidized bed in a static geometry (RFB-SG) observed at different solids loadings is shown in Figure 3. At low solids loadings (0.2 kg in Figure 3), a quite uniform dilute rotating fluidized bed is observed. The particle motion is complex and collisions between the particles and the solid walls, mainly the outer cylindrical side wall, of the fluidization chamber are important. Due to the centrifugal force, the gas-solids separation is, however, excellent with no particle losses via the chimney outlet. As the solids loading increases (0.3 kg - 0.5 kg, not shown in Figure 3), particle-particle collisions become more important and, as a result of the centrifugal force, a densification, i.e. an accumulation of particles, near the cylindrical side wall of the fluidization chamber is observed. A dense particle bed forms near the outer cylindrical wall of the fluidization chamber. More inwards, the particle bed gradually becomes less dense and the gas-solids separation remains excellent with no particle losses via the chimney. At solids loadings of 0.3 kg - 0.5

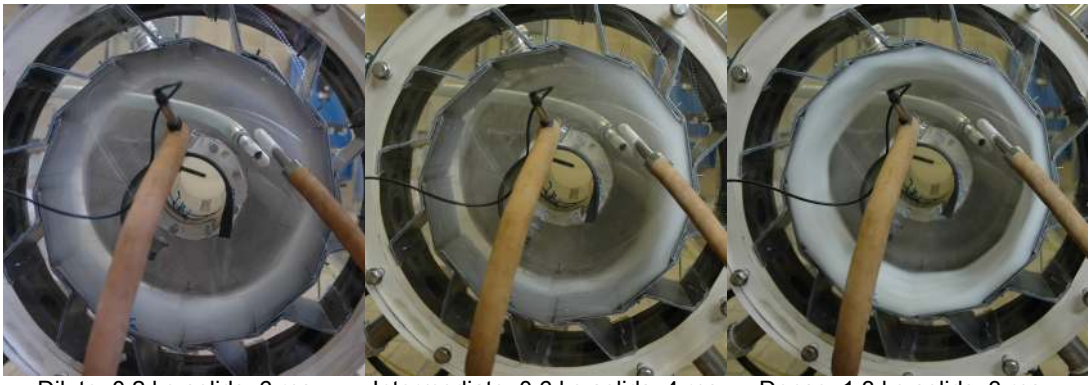

Dilute: 0.2 kg solids, 6 rps Intermediate: 0.6 kg solids, 4 rps Dense: 1.3 kg solids, 3 rps

Figure 3: 1G-Geldart D particles: polymer, $<d_p>$ = 2-5 mm (cylinders), ρ_p = 950 kg m^{-3}. Horizontal operation. Total gas flow rate: 0.2 m^3 s^{-1}. Conditions: see Table 1 a).

kg, channeling may occur (not shown; shown for the Alumina particles further in this paper). In such case, the particles rotate preferentially at one side, i.e. near one of the end plates, of the fluidization chamber and the gas bypasses via the other side,

i.e. near the other end plate of the fluidization chamber. Hence, the particle distribution is strongly non-uniform in the longitudinal direction of the fluidization chamber. In case channeling occurs, the particle bed height increases locally and, as a result, close to the end plate, where the increase of the bed height is the most pronounced, particle losses via the chimney outlet may occur. This may disturb further filling of the fluidization chamber with particles and limit as such the solids hold-up in the fluidization chamber. Channeling is enhanced as there is no controlled uniform distribution of the gas flow rate over a gas inlet slot. Only the total gas flow rate is controlled in the experiment.

As the solids loading increases further (0.6 kg in Figure 3), slugging is observed (probably corresponding to an eigenmode of the system). The solids are distributed evenly in the longitudinal direction of the fluidization chamber, but a strongly non-uniform tangential distribution of the solids in the fluidization chamber occurs, i.e. a solids slug rotates in the fluidization chamber. As with channeling, gas bypassing dense particle zones enhances slugging. In the experiment, only the total gas flow rate is controlled and not the distribution of the gas flow rate over the different gas inlet slots. As a result, in the slugging regime, the gas flow rate through a gas inlet slot drops sharply when the solids slug passes by, the gas entering the fluidization chamber preferentially via the other gas inlet slots that do not face the resistance of a solids bed. Slugging is most probably related to a poor radial fluidization of the particle bed.

At higher solids loadings and provided that the bed rotational speed is sufficiently high (1.3 kg in Figures 3 and 4), slugging disappears and the polymer particles form a stable, dense, uniform rotating fluidized bed. This transition is quite abrupt. The snap-shot in Figure 4 may give the impression of a (rotating) fixed bed, as obtained in conventional rotating fluidized beds below the minimum fluidization gas flow rate, but the particle bed is (mainly tangentially) fluidized and, as seen from Figure 3 with a larger exposure time, the particle motion is complex and vigorous. As a result of the combination of the tangential and some radial motion, the particles are well-mixed. The assumption of a solid body rotation of the particle bed seems, however, justified. With the current fluidization chamber design, at high solids loadings, the radial fluidization or bed expansion with the polymer particles is rather limited, despite the high radial fluidization gas velocities (radial gas-solid slip velocities of at

Dense: 1.3 kg solids, 3 rps

Figure 4: Conditions: see Figure 3 and Table 1 a).

least 2 m s^{-1}). In fact, the detail snap-shot in Figure 4 shows that the freeboard of the rotating fluidized bed only is truly radially fluidized, in agreement with the layered fluidization observed in conventional rotating fluidized beds (10,11). Hence, for the polymer particles (Table 1 a)), with the current fluidization chamber design, the ratio

of the tangential and the radial velocities, so i.e. the ratio of the centrifugal force and the radial drag force, is too high and the radial gas velocity is close to the surface minimum fluidization velocity. As a result, the gas-solid separation is very good with no particle losses via the chimney.

FLUIDIZATION BEHAVIOR WITH ALUMINA PARTICLES

Figure 5 shows the rotating fluidized bed behavior obtained with the Alumina 1G-Geldart B - type particles at different solids loadings. The operating conditions and particle properties are summarized in Table 1 b). During the experiment, the solids outlet is closed, allowing to set the solids loading in the fluidization chamber more easily.

At low solids loadings (0.15 kg in Figure 5), channeling, i.e. gas bypassing zones of higher solids density, occurs, resulting in a longitudinally strongly non-uniform rotating fluidized bed. The solids are seen to rotate at one side of the fluidization chamber, close to the end plate in the back in Figure 5, whereas the gas is bypassing via the other side of the fluidization chamber. The role of the solids feeder design in the occurrence of channeling is to be further investigated, but most probably channeling in a certain low solids loading range is intrinsic to the rotating fluidized bed in a static geometry.

At higher solids loadings (0.8 kg and 1.0-1.5 kg in Figure 5), the solids are longitudinally more evenly distributed. The rotating fluidized bed behavior at higher solids loadings is very different with the Alumina particles (Figure 5) than with the polymer particles (Figures 3 and 4). With the Alumina particles, the rotating fluidized bed is less dense and less uniform than with the polymer particles and bubble formation is observed. Furthermore, the rotating fluidized bed is much more agitated and the radial fluidization is much more pronounced. As a result of the radial bed expansion, the freeboard of the rotating fluidized bed is positioned rather close to the chimney and particle losses via the chimney outlet are quite pronounced with the Alumina particles, whereas absent with the polymer particles. Hence, although the solids outlet is closed in the experiment, continuous solids feeding is necessary to

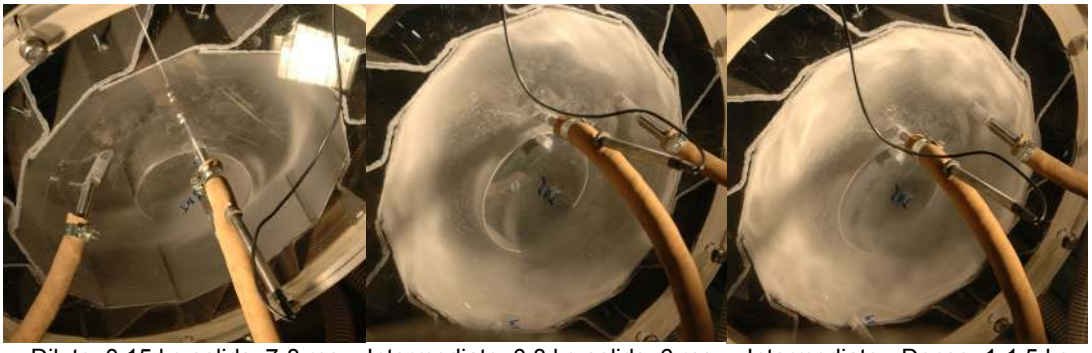

Dilute: 0.15 kg solids, 7-8 rps | Intermediate: 0.8 kg solids, 6 rps | Intermediate - Dense: 1-1.5 kg solids, 3-4 rps

Figure 5: 1G-Geldart B particles: Alumina, $<d_p>$ = 400 µm (*), ρ_p = 2100 kg m^{-3}. Horizontal operation. Total gas flow rate: 0.2 m^3 s^{-1}. Conditions: see Table 1 b).
(*) In the fluidization chamber; 300 µm for the original Alumina particles fed.

operate the fluidization chamber at a constant solids loading. After keeping the solids loading in the fluidization chamber constant at about 1.5 kg over a 10 min period, roughly 2.5 kg solids are recuperated via the cyclone and the filter. The particle residence time is, however, difficult to determine. Based on the visual observations,

The 12th International Conference on Fluidization - New Horizons in Fluidization Engineering, Art. 70 [2007]

the particle residence time distribution is believed to be broad and complex. Accurate particle residence time measurements are to be carried out.

CONCLUSIONS

The new concept of a rotating fluidized bed in a static geometry (1) is presented and experimentally investigated using one and the same fluidization chamber design with either large diameter, low density polymer particles or small diameter, higher density Alumina particles, at different solids loadings, and in vertical and horizontal operation. In all cases, a rotating fluidized bed and a reasonable to good gas-solid separation can be obtained, provided that the rotational speed is sufficiently high, that is the gas flow rate is sufficiently high. The behavior of the rotating fluidized bed is, however, very different for the polymer and the Alumina particles, in particular at higher solids loadings. Whereas the polymer particles tend to form a dense uniform bed, the Alumina particles tend to form a less dense and less uniform bed.

ACKNOWLEGMENTS

Prof. Jamal Chaouki at Total Petrochemicals (Feluy - Belgium) is greatly acknowledged for his interest in this work and for the helpful discussions.

REFERENCES

1. de Broqueville Axel : Catalytic polymerization process in a vertical rotating fluidized bed : Belgian Patent 2004/0186, Internat. Classif. : B01J C08F B01F; publication number : 1015976A3
2. Quevedo JA, Nakamura H, Shen Y, Dave RN, Pfeffer R. Fluidization of nanoparticles in a rotating fluidized bed. *Proceedings of AIChE Annual meeting 2005*. Cincinnati, OH, USA; 2005.
3. Ahmadzadeh A, Arastoopour H, Teymoour F. Rotating fluidized bed an efficient polymerization reactor. *Proceedings of AIChE Annual meeting 2005*. Cincinnati, OH, USA; 2005.
4. Qian G-H, Burdick IW, Pfeffer R, Shaw H, Stevens JG. Soot removal from diesel engine exhaust using a rotating fluidized bed filter. *Advances in Environmental Research* 2004; 8: 387-395.
5. Watano S, Nakamura H, Hamada K, Wakamatsu Y, Tanabe Y, Dave RN, Pfeffer R. Fine particle coating by a novel rotating fluidized bed coater. *Powder Technol*. 2004; 141: 172-176.
6. Watano S, Imada Y, Hamada K, Wakamatsu Y, Tanabe Y, Dave RN, Pfeffer R. Microgranulation of fine powders by a novel rotating fluidized bed granulator. *Powder Technol*. 2003; 131: 250-255.
7. Qian G-H, Bagyi I, Burdick IW, Pfeffer R, Shaw H, Stevens JG. Gas-solid fluidization in a centrifugal field. *AIChE J*. 2001; 47(5): 1022-1034.
8. Qian G-H, Bágyi I, Pfeffer R, Shaw H, Stevens JG. A parametric study of a horizontal rotating fluidized bed using slotted and sintered metal cylindrical gas distributors. *Powder Technol*. 1998; 100: 190-199.
9. Qian G-H, Bágyi I, Pfeffer R, Shaw H, Stevens JG. Particle mixing in rotating fluidized beds: Inferences about the fluidized state. *AIChE J*. 1999; 45(7): 1401-1410.
10. Chen Y-M. Fundamentals of a centrifugal fluidized bed. *AIChE J*. 1987; 33(5): 722-728.
11. Fan LT, Chang CC, Yu YS, Takahashi T, Tanaka Z. Incipient fluidization condition for a centrifugal fluidized bed. *AIChE J*. 1985; 31(6): 999-1009.